

Determination of equilibrium coupling angles in magnetic multilayers by polarized neutron reflectometry

C. H. Marrows,^{1,*} S. Langridge,² and B. J. Hickey¹

¹*Department of Physics and Astronomy, E.C. Stoner Laboratory, University of Leeds, Leeds LS2 9JT, United Kingdom*

²*ISIS Facility, Rutherford Appleton Laboratory, Chilton, Didcot, Oxon OX11 0QX, United Kingdom*

(Received 14 January 2000; revised manuscript received 24 May 2000)

We have performed polarized neutron reflectometry (PNR) on Co/Cu multilayers grown by sputter deposition at the first antiferromagnetic (AF) maximum of the coupling oscillation. The growth of the Cu spacer layers was paused halfway through each layer for a variable amount of time to allow residual gases to be adsorbed onto the surface. A sample with clean Cu spacers shows good AF coupling, with low remanence and high saturation field. The PNR spectra show a strong $\frac{1}{2}$ -order Bragg peak and little splitting between the reflectivities for incident \uparrow and \downarrow spin neutrons at zero field, characteristic of AF ordering. Meanwhile, a more heavily gas-damaged sample with a remanent fraction of $\sim\sqrt{2}/2$ has strongly spin-split PNR spectra at the critical edge and nuclear Bragg peak, showing a significant ferromagnetic component. A strong $\frac{1}{2}$ -order Bragg peak is still present. We are able to fit accurately the magnetization and PNR data by assuming that such a sample shows considerable biquadratic coupling, with moments coupled close to 90° at zero field.

One of the most striking properties of the new generation of magnetic multilayer structures is the presence of antiferromagnetic¹ (AF) or oscillatory² indirect exchange coupling between magnetic layers on either side of a thin nonmagnetic spacer. The oscillation in coupling with spacer thickness is due to the quantum interference of spin-polarized wave functions,³ with the ferromagnet/spacer interfaces acting analogously to a Fabry-Perot *étalon* with spin-dependent reflection coefficients. A variety of theoretical methods have been employed to attempt to calculate these reflection coefficients, such as RKKY-like theories,⁴ total energy calculations,⁵ and quantum confinement of spin- \downarrow holes.⁶ These various theories have enjoyed increasing success in predicting the period, amplitude, and temperature dependence of the coupling.

We have been studying the interlayer coupling of one multilayer system, Co/Cu, as it exhibits a large giant magnetoresistance (GMR) which is of particular scientific and technological interest.⁷ We previously found that relatively low levels of residual gas in the vacuum chamber during growth would significantly reduce the GMR ratio of Co/Cu multilayers while not affecting the resistivity of the films. The most damaging point at which these gases could enter the multilayer stack was in the bulk of the Cu spacer layers.⁸ This was explained by a reduction of the degree of antiferromagnetic character in the interlayer coupling. Subsequently it became apparent that a plausible explanation for the reduction of GMR would be a smooth rotation of the equilibrium (zero-field) angle between adjacent moments from π to 0 as the base pressure of the system worsened.⁹ This noncollinear ordering of the moments requires the introduction of a significant biquadratic term in the expression for the free energy of the multilayer. We found that the introduction of this biquadratic term would correctly reproduce the experimentally observed dependences of the magnetization and GMR on field and on each other across the width of the first AF peak in the coupling oscillation.¹⁰ Such noncollinear coupling has now been observed in a number of dif-

ferent material systems, e.g., Fe/Cr,¹¹ NiFe/Ag,¹² and Co/Cu.¹³ It may be described phenomenologically by the inclusion of the biquadratic second term in the expansion in powers of $\mathbf{S}\cdot\mathbf{S}$ of the indirect exchange interaction between spins \mathbf{S} in adjacent magnetic layers. The free energy per unit area, ϵ , of a Co/Cu/Co trilayer in applied field H may be written as

$$\epsilon = -\mu_0 m H t (\cos \theta_1 + \cos \theta_2) - J_1 \cos \Theta - J_2 \cos^2 \Theta, \quad (1)$$

where the Co layers are of magnetization m and thickness t . The moments make angles θ with the field and Θ with each other, i.e., $\Theta = \theta_1 - \theta_2$. The interlayer exchange appears in the form of the bilinear and biquadratic coupling constants J_1 and J_2 . The biquadratic term represents non-Heisenberg exchange. Such coupling appears to be commonplace in a variety of multilayer systems.¹⁴ With the proper sign for J_2 the two energy minima can be found at $\Theta = \pm \pi/2$, leading to orthogonal ordering of adjacent layer moments. By introducing J_1 it is possible to close up (for $J_1 > 0$) or force apart (for $J_1 < 0$) the moments to reach any zero-field equilibrium angle between 0 and π . An appropriate variation of J_1 and J_2 can therefore yield the proper decline in GMR and AF coupling with rising base pressure in the sputtering chamber.

In this paper we report the results of polarized neutron reflectometry¹⁵ (PNR) performed on such samples. Among the many applications found for this technique, one of the most common is determining the magnetic alignments in multilayer structures,¹⁶ acting in many respects as a depth-selective vector magnetometer. It is therefore suited to investigating the nature of the angular dependence of the exchange interaction between the Co layers in these multilayers.

The samples were deposited by dc magnetron sputtering on 25 mm \times 25 mm pieces of Si (001) wafer. The working gas pressure was 3.0 mTorr. The multilayers were nominally of the form {Co(10 Å)/(Cu(9 Å)) \times 25}. This Cu thickness corresponds to the first antiferromagnetic maximum in the

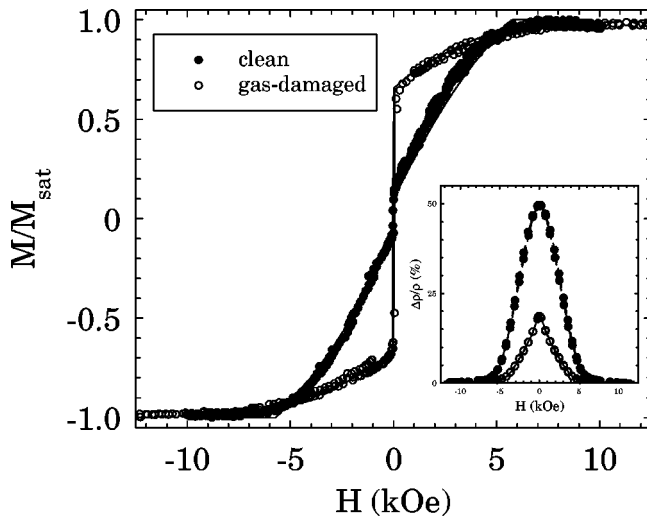


FIG. 1. Magnetization loops for the two multilayers. The solid lines are fits to the data. The inset is magnetoresistance measurements for nominally identical smaller samples grown in the same vacuum cycle.

oscillatory exchange coupling. The lowest base pressure of the system is achieved by cooling a Meissner coil with liquid nitrogen—it is possible to raise the base pressure by not fully cooling the coil. This mainly results in a higher partial pressure of H_2O . One sample was prepared with each layer grown continuously, in a system base pressure of 2.0×10^{-8} Torr. The growth was paused for 30 s in the middle of each Cu spacer layer in the second sample, exposing the surface to a base pressure of 1.3×10^{-7} Torr. Both samples were prepared in the same vacuum cycle of the system.

Structural characterization of the samples was performed by low-angle x-ray reflectometry. Magnetization loops were measured by means of the magneto-optic Kerr effect (MOKE). Magnetoresistance was measured by a four-probe dc method. PNR was carried out on the CRISP time-of-flight reflectometer at ISIS.^{17–19} The instrument was operated without analysis of the spins of the exit beam of neutrons, and magnetic fields were applied to the sample with an electromagnet. A minimum applied field of 50 Oe is required to prevent depolarization of the neutron beam. All measurements were performed at room temperature.

In Fig. 1 we show the magnetization loops for the two different samples. It is immediately apparent from the low remanence that the clean sample has substantial AF ordering at low fields. Meanwhile, the remanence of the gas-damaged sample is substantial, approximately 0.65 of the saturated magnetization. As expected the GMR of the sample with the small remanence is much higher; indeed it is just over double. However, the resistivity of the two samples when magnetically saturated is very similar, $20 \pm 2 \mu\Omega$ cm at room temperature.

It is of course possible to explain these changes in two ways. The gas-damaged sample may consist of perfect AF regions, interspersed with regions where the moments lie parallel to each other that contribute nothing to the GMR. On the other hand, we may set the moments at an angle to each other, which will provide a net moment at remanence, but also some misalignment that gives rise to GMR as the moments are closed together by an external field. It is noteworthy

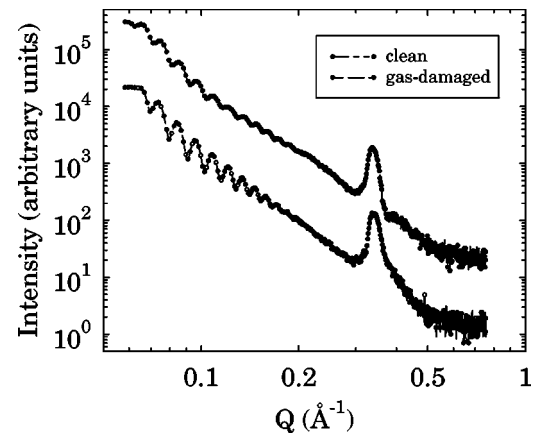


FIG. 2. Low-angle x-ray diffraction spectra for the two multilayers. The Bragg peak at $Q \approx 3.2 \text{ \AA}^{-1}$ is due to the chemical periodicity of the multilayer. The two scans are offset by a decade of intensity for clarity.

thy that if we were to choose angles of π for the clean sample and $\pi/2$ for the gas-damaged sample, this would yield a GMR ratio in the clean sample of double that in the gas-damaged one, while simultaneously yielding remanences of zero and $\sqrt{2}/2$ (≈ 0.7), respectively. It should also be noted that changes in anisotropy cannot account for the differences in magnetic response we see here—generally these affect the nature of the hysteresis in the magnetization loop.⁹

In Fig. 2 low-angle x-ray reflectivity spectra are displayed. Since each sample has an area similar in size to the racetrack of the magnetron sputter guns, we might expect that the samples are not perfectly uniform in thickness, and x-ray scans were taken at 2.5 mm intervals across the sample. (The particular scans shown are from the center of the wafer.) All the scans are very similar, although the value of Q at which the bilayer Bragg peak is observed is slightly higher at the edges of the sample, corresponding to a slightly thinner layer. For the clean sample the mean bilayer spacing is 19.4 \AA with a standard deviation across the wafer of 0.6 \AA . For the gas-damaged sample the mean is 19.1 \AA , again with a standard deviation of only 0.6 \AA . A fuller structural analysis of similar samples was previously presented:²⁰ the multilayers were found to be extremely smooth, with rms roughnesses of $\sim 1 \text{ \AA}$ and a very high degree of vertical correlation of the interfaces.

PNR produces very rich data sets, the most important of which are displayed in Figs. 3 and 4. In these two figures we show the 50 Oe data for the two samples. Although it is not possible to perform PNR in field-free conditions due to loss of polarization of the neutron beam, 50 Oe can be seen to be only a weak perturbation of the state of these samples, where the saturation fields are much higher (see Fig. 1). The spin- \uparrow and \downarrow labels refer to the polarization of the incident neutron beam. There are several features common to both data sets, such as the Bragg peaks, critical edges, and finite-size fringes. For very low Q , total internal reflection of the neutrons occurs and the reflectivity is unity. All the data have been normalized in reflectivity to this point. Above the critical value of Q the neutrons penetrate the sample. Bragg reflection occurs at certain values of Q corresponding to periodicities within the sample. The first-order Bragg peak at $Q = 0.32 \text{ \AA}^{-1}$ is due to the chemical periodicity of the

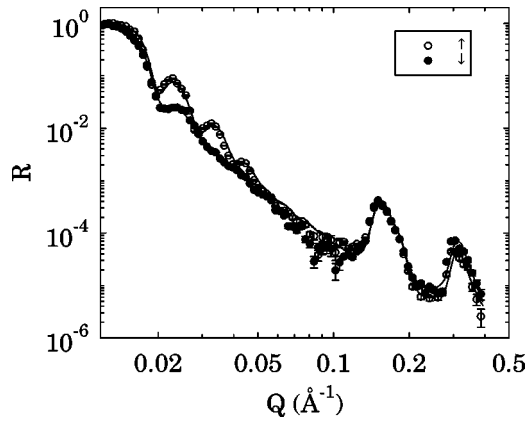


FIG. 3. Polarized neutron reflectometry spectra for the clean antiferromagnetically coupled sample at $H=50$ Oe. The data are the points; the solid lines are the results of the simulation.

sample, and yields a bilayer spacing of 19.6 \AA , close to the nominal value. Meanwhile the $\frac{1}{2}$ -order peak at $Q=0.16 \text{ \AA}^{-1}$ corresponds to a doubling of the real space period and is due to the AF ordering of the sample, leading to a magnetic period twice that of the chemical period. The magnetic origin of the peak is confirmed by its suppression as the applied magnetic field is increased, vanishing above the saturation field when all the moments are closed and no AF order persists. Meanwhile, the fringes visible in both scans below $Q=0.1 \text{ \AA}^{-1}$ are analogous to Kiessig fringes observed in low-angle x-ray reflectivity spectra, arising due to interference of the beams reflected at the air/multilayer and multilayer/substrate interfaces.

There are a number of important differences between the two samples. In Fig. 3 the two spectra are only weakly spin split, with the only splitting of any significance in the finite-size fringes. Meanwhile, in Fig. 4 there is significant splitting both at the critical edge and at the first-order Bragg peak. These are characteristic of a sample with a significant ferromagnetic component. The $\frac{1}{2}$ -order peak is not split as it is due to AF ordering, which, without polarization analysis, cannot exhibit any spin dependence.

As the field is increased all these features become more pronounced: spin splitting of the critical edge, at the first-order Bragg peak, and of the finite-size fringes, and a sup-

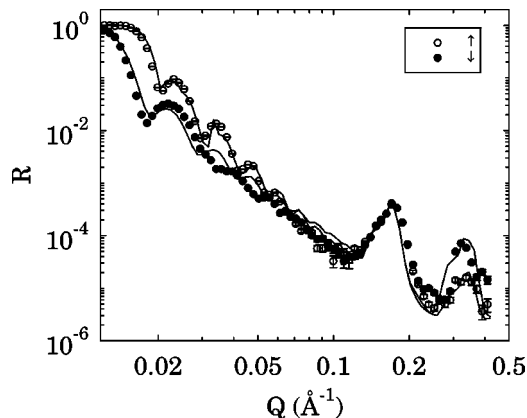


FIG. 4. Polarized neutron reflectometry spectra for the gas-damaged noncollinearly coupled sample at $H=50$ Oe. The data are the points; the solid lines are the results of the simulation.

pression of the $\frac{1}{2}$ -order peak. The data set of Fig. 4 is qualitatively very similar to that of the clean sample in a field roughly halfway to saturation, i.e., when the moments are partly closed together. Both samples behave in a comparable manner when saturated, and are thus entirely in ferromagnetic alignment. In this case the $\frac{1}{2}$ -order Bragg peak is entirely absent, and the critical edge, finite-size fringes, and first-order peak are strongly spin split.

The four spin-dependent cross sections were simulated using an optical potential-type model²¹ and combined to produce the spin-dependent specular reflectivity. The calculations were then numerically convoluted with the instrumental resolution. We averaged over two different sets of input parameters in order to account for the slight nonuniformity in thickness of the sample. In this model we assume that all the intensity measured is due to specular scatter, with zero diffuse component. We have recently measured the off-specular scatter from several magnetic multilayers using the ^3He multidetector on CRISP.²² In the case of these samples, where the coupling is strong, we find little diffuse scatter, even at zero field—a weak diffuse component is just discernible under the instrument-broadened $\frac{1}{2}$ -order Bragg peak. We therefore feel justified in neglecting this very weak scatter and treating all the intensity as entirely specular.

The Co moment is found to be $\sim 1.5\mu_B/\text{atom}$, a little lower than the bulk value of $1.7\mu_B/\text{atom}$. This is not so surprising given the extreme thinness of the films, which will suppress both the magnetization and the Curie point.²³ The value for the zero-field coupling angle Θ for the gas-damaged sample giving the best fit was 86° , while for the clean sample $\Theta = 170^\circ$. The splitting in the finite-size fringes seen in Fig. 3 can be reproduced by assuming that the first few Co layers deposited on the substrate form a ferromagnetic block. Cross-sectional transmission electron micrographs of similar samples confirm that the layering quality is poor for the first few bilayer repeats,⁹ so we should expect that the AF interlayer coupling in this region should be significantly impaired.

It is now possible to take the thickness and magnetization values determined from the PNR and simulate the expected magnetic response of the samples. Setting $t=9.75 \text{ \AA}$ and $m=1.25 \text{ MA m}^{-1}$, and following the path of minimum ϵ , as given by Eq. (1), as a function of H , it is possible to obtain the simulated magnetization loops of best fit shown as solid lines in Fig. 1 using the following coupling constants: for the clean sample $J_1 = -0.15 \text{ mJ m}^{-2}$, $J_2 = -0.085 \text{ mJ m}^{-2}$; for the gas-damaged sample $J_1 = -0.024 \text{ mJ m}^{-2}$, $J_2 = -0.17 \text{ mJ m}^{-2}$. [Note that these values include the factor of 2 correction required to transfer the trilayer model of Eq. (1) to a multilayer.] This leads to equilibrium values of Θ of 82° and 180° , respectively, close to the values giving the best fits to the PNR data. The small remanence in the clean sample comes entirely from the ferromagnetic block of five layers at the bottom of the stack in this simulation.

To conclude, we have studied by PNR the magnetic properties of multilayers exhibiting good AF coupling, and a form of coupling intermediate between AF and ferromagnetic. The sample shows characteristics of both AF coupling (high saturation field, appreciable GMR, and strong $\frac{1}{2}$ -order PNR Bragg peak) and ferromagnetic coupling (high remanence, spin-split PNR critical edge, and first-order Bragg

peak). This suggests that some sort of mixed coupling is present. The width of the PNR Bragg peaks in Figs. 3 and 4 yields a vertical magnetic coherence length comparable with the size of the multilayer, so that the fluctuations in coupling must be lateral. This means that there is the opportunity for noncollinear ordering of adjacent layer moments, as described in the well-known Slonczewski coupling fluctuation model of biquadratic exchange,²⁴ where different lateral regions of the spacer have positive or negative coupling energies. When the lateral length scale of the fluctuations in coupling strength is comparable to the exchange length of the magnetic layers, then the magnetization cannot simultaneously satisfy adjacent regions of opposite coupling. An equilibrium angle is found partway between 0 and π , leading to a noncollinear arrangement of moments. On the other hand, if the lateral fluctuations are long ranged, then the layers can break into domains such that the coupling conditions are locally satisfied everywhere. It is possible that as the

residual gases accumulate on the sample surface during pauses in growth they clump in particular areas, and cause a change in sign of J_1 from negative to positive. If these areas were small compared to the exchange length, i.e., only 1 or 2 nm across, then this could lead to mixed coupling of the type that will cause a biquadratic term in the Slonczewski model, and is also consistent with the gradual decrease in Θ from π to zero as reported in Ref. 9. We know from Lorentz microscopy studies that on dc demagnetization the samples are in a single domain state,⁹ and the good agreement between the simulations and the PNR data is further compelling evidence that there is substantial biquadratic coupling in these gas-damaged samples.

C.H.M. would like to thank the Royal Commission for the Exhibition of 1851 for financial support. We are grateful to the Rutherford Appleton Laboratory for the provision of beam time at ISIS.

*Email address: c.marrows@leeds.ac.uk

¹P. Grünberg, R. Schrieber, Y. Pang, M.B. Brodsky, and H. Sowers, Phys. Rev. Lett. **57**, 2442 (1986).

²S.S.P. Parkin, N. More, and K.P. Roche, Phys. Rev. Lett. **64**, 2304 (1990).

³P. Bruno, Phys. Rev. B **52**, 411 (1995).

⁴P. Bruno and C. Chappert, Phys. Rev. B **46**, 261 (1992).

⁵M. van Schilfgaarde and F. Herman, Phys. Rev. Lett. **71**, 1923 (1993).

⁶J. Mathon, D.M. Edwards, R.B. Muniz, and M.S. Phan, Phys. Rev. Lett. **67**, 493 (1993).

⁷S.S.P. Parkin, R. Bhadra, and K.P. Roche, Phys. Rev. Lett. **66**, 2152 (1991).

⁸C.H. Marrows, B.J. Hickey, M. Malinowska, and C. Mény, IEEE Trans. Magn. **33**, 3673 (1997).

⁹C.H. Marrows, B.J. Hickey, M. Herrmann, S. McVitie, J.N. Chapman, T.P.A. Hase, B.K. Tanner, M. Ormston, and A.K. Petford-Long, Phys. Rev. B **61**, 4131 (2000).

¹⁰C.H. Marrows and B.J. Hickey, Phys. Rev. B **59**, 463 (1999).

¹¹M. Rührig, R. Schäfer, A. Hubert, R. Mosler, J.A. Wolf, S. Demokritov, and P. Grünberg, Phys. Status Solidi A **125**, 635 (1991).

¹²S. Young, B. Dieny, B. Rodmacq, J. Mouchot, and M.H. Vaudaine, J. Magn. Magn. Mater. **162**, 38 (1996).

¹³Z.J. Yang and M.R. Scheinfein, IEEE Trans. Magn. **31**, 3921 (1995).

¹⁴S.O. Demokritov, J. Phys. D **31**, 925 (1998).

¹⁵J.F. Ankner and G.P. Felcher, J. Magn. Magn. Mater. **200**, 741 (1999).

¹⁶G.P. Felcher, Physica B **268**, 154 (1999).

¹⁷A. Schreyer, J.F. Ankner, Th. Zeidler, H. Zabel, C.F. Majkrzak, M. Schäfer, and P. Grünberg, Europhys. Lett. **32**, 595 (1995).

¹⁸S. Adenwalla, G.P. Felcher, E.E. Fullerton, and S.D. Bader, Phys. Rev. B **53**, 2474 (1996).

¹⁹R. Felici, J. Penfold, R.C. Ward, and W.G. Williams, Appl. Phys. A: Solids Surf. **45**, 169 (1988).

²⁰C.H. Marrows, N. Wisser, B.J. Hickey, T.P.A. Hase, and B.K. Tanner, J. Phys.: Condens. Matter **11**, 81 (1999).

²¹S.J. Blundell and J.A.C. Bland, Phys. Rev. B **46**, 3391 (1992).

²²S. Langridge, J. Schmalian, C.H. Marrows, D.T. Dekadjevi, and B.J. Hickey, J. Appl. Phys. **87**, 5750 (2000).

²³C.H. Marrows, R. Loloee, and B.J. Hickey, J. Magn. Magn. Mater. **184**, 137 (1998).

²⁴J.C. Slonczewski, Phys. Rev. Lett. **67**, 3172 (1991).